LC/MS analysis of stratum corneum lipids: ceramide profiling and discovery[S]

Jeroen van Smeden,* Louise Hoppel,[†] Rob van der Heijden,[†] Thomas Hankemeier,[†,§] Rob J. Vreeken,[†,§] and Joke A. Bouwstra[1,*]

Division of Drug Delivery Technology,* Division of Analytical Biosciences,[†] and Netherlands Metabolomics Centre,[§] Leiden/Amsterdam Center for Drug Research, Leiden, The Netherlands

Abstract **Ceramides (CERs) in the upper layer of the skin, the stratum corneum (SC), play a key role in the skin barrier function. In human SC, the literature currently reports 11 CER subclasses that have been identified. In this paper, a novel quick and robust LC/MS method is presented that allows the separation and analysis of all known human SC CER subclasses using only limited sample preparation. Besides all 11 known and identified subclasses, a 3D multi-mass chromatogram shows the presence of other lipid subclasses. Using LC/MS/MS with an ion trap (IT) system, a Fourier transform-ion cyclotron resonance system, and a triple quadrupole system, we were able to identify one of these lipid subclasses as a new CER subclass: the ester-linked ω-hydroxy fatty acid with a dihydrosphingosine base (CER [EOdS]). Besides the identification of a new CER subclass, this paper also describes the applicability and robustness of the developed LC/MS method by analyzing three (biological) SC samples: SC from human dermatomed skin, human SC obtained by tape stripping, and SC from full-thickness skin explants. All three biological samples showed all known CER subclasses and slight differences were observed in CER profile.**—van Smeden, J., L. Hoppel, R. van der Heijden, T. Hankemeier, R. J. Vreeken, and J. A. Bouwstra. **LC/MS analysis of stratum corneum lipids: ceramide profiling and discovery.** ***J. Lipid Res.*** **2011.** 52: **1211–1221.**

Supplementary key words liquid chromatography • mass spectrometry • sphingolipids • human skin lipids • normal-phase liquid chromatography • atmospheric pressure chemical ionization mass spectrometry • identification • 3D multi-mass chromatogram

The outermost layer of mammalian skin, the stratum corneum (SC), consists of corneocytes embedded in a lipid matrix. This layer serves as the main barrier for diffusion of substances across the skin. As the lipid matrix is the only continuous pathway in the SC, the composition and organization of these lipids are of major importance for a competent skin barrier function (1–4). The major lipid classes in human SC are cholesterol, free fatty acids, and ceramides (CERs). In particular, the CERs have drawn much attention and several reported studies demonstrate that changes in CER composition may play a role in an impaired skin barrier (5–11). The various CERs consist of a sphingoid base linked via an amide bond to a fatty acid. Both variations in the fatty acid carbon chain and the sphingoid base architecture result in a large number of CER subclasses with a wide variation in chain length distribution. The molecular architecture of these subclasses is depicted in **Fig. 1**. Over the years, important information about CER composition in human SC has been obtained using high performance thin layer chromatography (HPTLC) in conjunction with NMR. This resulted in a gradual increase in the number of identified subclasses. By use of these methods, nine different human CER subclasses have been identified in the SC of healthy human skin (12–16). As HPTLC is easily accessible, it is still frequently used in various fields with respect to skin lipid research to determine the CER subclasses in human SC (11, 17, 18). However, these approaches are very time consuming and a high quantity of material is required, which is not always available. The application of LC/MS results in a much more detailed profile of each individual subclass using only small quantities of material (19–28). Besides their important role in human skin, CERs are also key molecules with respect to cell signaling, growth, differentiation, and apoptosis (29–38). Also in these research areas, the intro-

The authors acknowledge Technologiestichting STW for financing this project (No. 10064) and Cosmoferm for the provision of the synthetic CERs. This study was also supported by the research program of the Netherlands Metabolomics Centre (NMC) which is part of The Netherlands Genomics Initiative/Netherlands Organization for Scientific Research.

Manuscript received 1 February 2011 and in revised form 22 March 2011.

Published, JLR Papers in Press, March 28, 2011
DOI 10.1194/jlr.M014456

Abbreviations: amu, atomic mass unit; APCI, atmospheric pressure chemical ionization; CER, ceramide; FT-ICR, Fourier transform ion cyclotron resonance; HPTLC, high performance thin layer chromatography; IT, ion trap; LOD, limit of detection; LOQ, limit of quantification; NPLC, normal-phase liquid chromatography; SC, stratum corneum; S/N, signal-to-noise ratio; TQ, triple quadrupole.

[1] To whom correspondence should be addressed.
e-mail: Bouwstra@chem.leidenuniv.nl

[S] The online version of this article (available at http://www.jlr.org) contains supplementary data in the form of one figure.

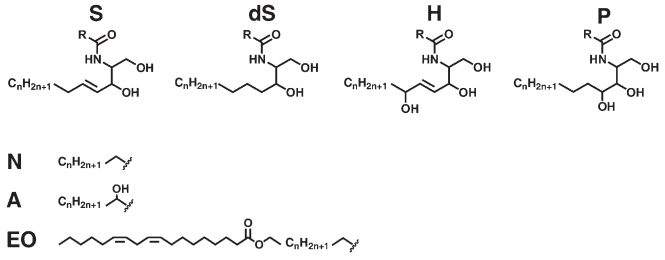

Fig. 1. Ceramide structures. Four possible sphingosine related chains (S, sphingosine; dS, dihydrosphingosine; H, 6-hydroxy-sphingosine; P, phyto-sphingosine) are linked via an amide bond to either of three different fatty acid components (N, nonhydroxy fatty acid; A, α-hydroxy fatty acid; EO, esterified ω-hydroxy fatty acid) resulting in, theoretically, 12 different CER subclasses. The literature has reported the presence of all but CER [EOdS] in human SC. R represents one of the three different fatty acid chains.

duction of MS has shown a tremendous boost in the identification of CERs in biological matrices.

With respect to human SC, two novel CER subclasses were reported recently (39), showing that the number of subclasses in human SC is still expanding. However, several of the LC/MS methods currently reported cannot analyze all CER subclasses in a single run. Also, almost all LC/MS methods reported so far are time consuming; multiple sample preparation steps are necessary and many methods require a solid phase extraction step beforehand. Moreover, the total analysis time of a single sample always exceeds 20 min and often more than 1 h, which is less attractive for analysis of a large number of samples. Therefore, the aims of our study were to *i*) minimize analysis time to allow quick sampling and analysis of total CER content, *ii*) use a minimal number of sample preparation steps to keep the method accessible while minimizing degradation during these steps, and *iii*) maintain a high CER sensitivity. To achieve these goals, we decided to use a normal phase liquid chromatography (NPLC) setup in combination with an atmospheric pressure chemical ionization (APCI) source. Regarding CER analysis, this choice offers some advantages over the commonly used reverse-phase LC combined with ESI-MS, such as *i*) considerably lower ion suppression (40–42), *ii*) APCI experiments are usually performed at higher flow rates compared with ESI, allowing for a shorter analysis time (43), and *iii*) APCI permits the use of a nonpolar mobile phase, enhancing the ionization efficiency for nonpolar compounds, i.e., CERs (in particular the higher mass subclasses) (21, 44).

Analysis of human SC CERs using this developed method resulted in the appearance of new lipid classes in a 3D-chromatogram. To obtain structural information about some of these new species, we performed fragmentation (MS/MS) on relevant ions (see Table 3), which led to the identification of one new CER subclass. The robustness of the LC/MS method was also demonstrated by measuring CERs from three different biological matrices: extracted lipids of isolated SC from native human skin, SC harvested with tape-strips, or SC obtained from the outgrowth of full-thickness human skin explants, referred to as the human skin explant model (45). We chose these three different biological matrices to demonstrate the applicability of this methodology for future studies.

MATERIALS AND METHODS

CER classification

In this paper, we use the most recently introduced CER classification system according to Motta et al. (46), which was extended by Masukawa et al. (39). The CERs consist of either a sphingosine (S), a phyto-sphingosine (P), a 6-hydroxy sphingosine (H) or a dihydrosphingosine (dS) base. This base is chemically linked to either a nonhydroxy fatty acid (N), α-hydroxy fatty acid (A), or an esterified ω-hydroxy fatty acid (EO). Current literature reports 11 different CER subclasses, viz., CERs denoted by [NS], [NdS], [NP], [NH], [AS], [AdS], [AP], [AH], [EOS], [EOP], and [EOH]. Figure 1 gives an overview of the molecular structures of all known CER subclasses. With respect to the fragmentation studies of CER species in this report, a more detailed nomenclature is used and shows as well, in parentheses, the number of carbon atoms for the specific ester, fatty acid, or carbon chain. For example, CER [E(18:2)O(30)S(18)] corresponds to a CER species containing a C_{18} sphingosine carbon backbone linked via an amide bond to a ω-hydroxy triacontanoic acid, which is ester-linked to a linoleic moiety.

Chemicals

Ethanol (EtOH), isopropyl alcohol (IPA), methanol (MeOH), and n-heptane of HPLC grade or higher were purchased from Biosolve (Valkenswaard, The Netherlands). HPLC grade chloroform was obtained from Lab-Scan (Dublin, Ireland). Ultra purified water was prepared using a Purelab Ultra purification system (Elga Labwater, High Wycombe, UK). Trypsin and trypsin inhibitor were purchased from Sigma-Aldrich Chemie Gmbh (Steinheim, Germany). Synthetic CER [N(24)dS(18)] was purchased from Avanti Polar Lipids (Alabaster, AL). All other synthetic CERs were kindly provided by Cosmoferm (Delft, The Netherlands): CER [EOS] (E(18:2)O(30)S(18)), CER [NS] (N(24)S(18)), CER [NP] (N(24)P(18)), CER [AS] (A(24)S(18)), CER [AP] (A(24)P(18)), and CER [EOP] (E(18:2)O(30)P(18)).

Isolation of SC from human skin, tape stripping, and cultured full-thickness explants

Within 24 h after surgery, residual subcutaneous fat was removed from the skin. The preparation of human SC was performed according to the procedure described by Nugroho et al. (47). In short, skin was stretched on Styrofoam and dermatomed to a thickness of around 300 μm (Deca Dermatome, DePuy Healthcare, Leeds, UK). Then, the skin was put on Whatman filters soaked in a solution of 0.1% trypsin in 150 mM PBS solution pH 7.4 (8 g/L NaCl, 2.86 g/L Na_2HPO_4, 0.2 g/L KH_2PO_4, 0.19 g/L KCl). After overnight storage at 4°C, the skin was incubated

TABLE 1. Applied LC gradient setup of a single run

Time (min)	A/B(%/%)
0.00	93/7
2.50	93/7
2.55	90/10
5.00	90/10
10.00	50/50
10.50	93/7
12.00	93/7

Solvent A corresponds to 100% heptane; Solvent B contains 50% heptane, 25% isopropanol, 25% ethanol.

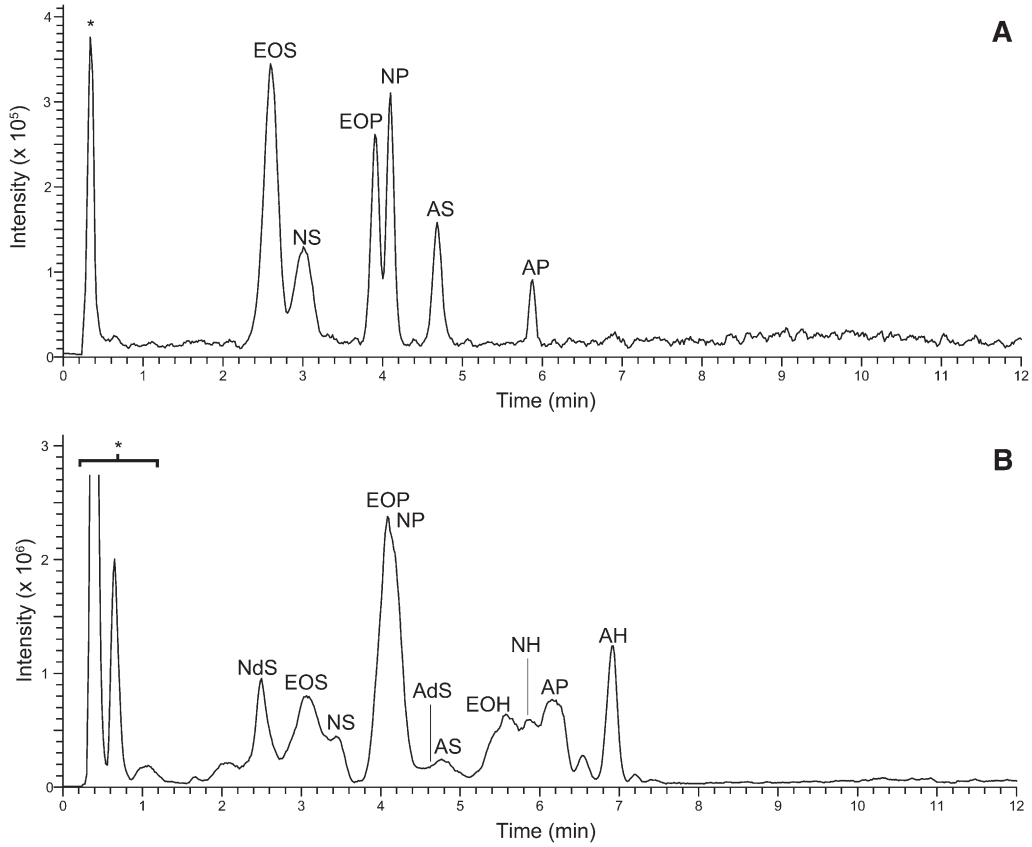

Fig. 2. NPLC-APCI-MS total ion current of (A) equimolar (250 fmol/CER) synthetic human CER mixture containing CER [EOS], [NS], [EOP], [NP], [AS], and [AP]; (B) crude lipid extract of human SC (abbreviations as in Fig. 1). Peaks noted with * contain other SC lipid classes (e.g., triglycerides, cholesterol) and do not interfere with the CER analysis.

for 1 h at 37°C followed by peeling off the SC from the epidermis. The SC was washed once in a 0.1% trypsin inhibitor in PBS pH 7.4 solution and twice in water and stored in a dry argon gas-containing environment to inhibit oxidation of the SC lipids. Lipids from the full-thickness skin explants model were also collected; six cultured samples were combined into two pools of three samples and treated analogous to the samples obtained from surgical skin described above, excluding the dermatome step. Lipids obtained from tape stripping were harvested according to the following procedure: tape stripping (area 4.5 cm^2) was performed on the ventral forearm of a healthy volunteer (male, age 33). Ten consecutive Poly(phenylene sulfide) tape strips (Nichiban, Tokyo, Japan) were taken at the same spot. All tapes were pressed to the targeted skin (450 g/cm^2) and peeled off with tweezers in one fluid stroke using alternating directions for each tape strip. The 5th to 8th tape strips were selected for lipid extraction. The tapes were punched to an area of 2 cm^2, and each punched area was put separately in a glass vial filled with 1 ml chloroform-MeOH-water (1:2:1/2). All vials were stored at −20°C under argon atmosphere.

Lipid extraction

Lipids from tape strips, SC isolated from dermatomed human skin, and cultured full-thickness skin explants were all extracted according to the method of Bligh and Dyer (48) with some small modifications described by Thakoersing et al. (49). Briefly, liquid-liquid extraction of the lipids from either human SC or tape strips was performed sequentially using three different ratios of solvent mixtures of chloroform-MeOH-water (1:2:1/2 ; 1:1:0 ; 2:1:0). A solution of 0.25 M KCl was added to extract polar lipids.

TABLE 2. Accurate mass LC/MS analysis and LOD/LOQ values of 6 synthetic ceramides

Ceramide	Main ion measured	Main ion mass measured (amu)[a]	LOD (fmol)[b]	LOQ (fmol)[b]
E(18:2)O(30)S(18)	$[M+H-H_2O]^+$	994.953	9	29
E(18:2)O(30)P(18)	$[M+H]^+$	1030.974	1	5
N(24)S(18)	$[M+H-H_2O]^+$	632.634	13	45
N(24)P(18)	$[M+H]^+$	668.655	18	60
A(24)S(18)	$[M+H-H_2O]^+$	648.629	28	94
A(24)P(18)	$[M+H]^+$	684.650	19	64
N(24)dS(18)	$[M+H]^+$	652.661	6	21

amu, atomic mass unit; LOD, limit of detection, defined as signal-to-noise ratio (S/N) = 3; LOQ, limit of quantification, defined as S/N = 10.

[a] Measured with FT-ICR MS, resolution 100.000.

[b] Measured with TQ MS: resolution full width at half maximum = 0.7 amu.

After drying to N_2 gas, lipids were dissolved in a solution of heptane-chloroform-MeOH: (95:2.5:2.5). Regarding the lipids isolated from SC of dermatomed skin, 1 ml of solvent was appropriate to obtain a proper sample concentration for optimal LC/MS analysis. SC lipid samples obtained from the four tape strips were pooled prior to drying and afterwards resolved in 0.1 ml to concentrate the lipids. Lipids extracted from cultured full-thickness skin explants were also resolved to a final volume of 0.1 ml.

CER analysis by LC/MS

NPLC was performed using a binary gradient solvent system of heptane (solvent A) and heptane/IPA/EtOH (2:1:1, solvent B) using a flow rate of 0.8 ml/min (see **Table 1** for detailed gradient description). Separation was performed using a polyvinyl alcohol (PVA)-Sil column (PVA-bonded column; 5 μm particle size, 100 × 2.1 mm i.d.) purchased from YMC (Kyoto, Japan). The HPLC (Alliance 2695, Waters Corp., Milford, MA) was coupled to one of several mass spectrometers, depending on the aim of the study. Additional details on the individual studies are described below. In general all mass spectrometers were equipped with an APCI source set to 450°C. Synthetic CERs had a final concentration ranging from nanomolar up to micromolar, depending on the experiment. Biological samples were concentrated to a final total lipid concentration around 0.1 mg/ml, determined by weighing. The injection volume of all samples was set to 10 μl. The analysis was performed using Thermo Finnigan Xcalibur software (version 2.0).

Profiling of CERs in synthetic and biological mixtures

Profiling of CERs in synthetic mixtures as well as in samples from dermatomed skin, tape strips, and full-thickness skin explants was performed with the LC system described above coupled to a triple quadrupole (TQ) mass spectrometer (TSQ Quantum, Thermo Finnigan, San Jose, CA) equipped with an APCI source operated in the positive ion mode. The temperature of the source heater was set to 450°C and the heated capillary was set to 250°C. The capillary voltage was maintained at 3 kV and the discharge current was set to 5 μA. The flow rates of the nitrogen sheath and auxiliary gas were set to 0.4 and 2.4 l/min, respectively. To obtain a full CER profile including all CER chain lengths, the scan range was set from 600–1200 atomic mass units (amu). The resolution full width at half maximum was set to 0.7 amu. The analysis time was set to 8 min with an additional 4 min of column washing and equilibration afterwards, leading to a total run time of 12 min. Synthetic CERs were used for development of the method, fragment analysis (see below), and limit of detection/limit of quantification (LOD/LOQ) determination. Regarding the development of the method, an equimolar synthetic mixture of 250 fmol/CER was prepared and analyzed. For LOD/LOQ determination, a range from micromolar to nanomolar was used, resulting in amounts on-column ranging from picomol to femtomol levels.

Identification of CER using (LC/)MS/MS

Fragmentation spectra (MS/MS) of synthetic CERs and human SC CERs were obtained using an ion trap (IT) system (LCQ Deca, Thermo Finnigan) combined with a Surveyor LC system (Thermo Finnigan). Synthetic CERs were infused (in chloroform-methanol 2:1) using a postcolumn low dead volume T-piece at a rate of 5 μL/min while maintaining a continuous flow of solvent A:B (93:7), as described above, at 0.8 ml/min. The normalized collision energy for MS/MS was set between 40% and 70%, depending on the specific fragments, which appeared to be indicative of a specific CER structure (more detail below). The sheath gas and auxiliary gas were set to consecutively 50 and 5 AU, which were slightly different settings compared with the setup used for general profiling of CERs described earlier but showed better results with respect to fragmentation of CERs. The scan time was set to 50 ms. All other parameters were similar to the setup of the TQ system described above. A drawback of MS/MS using an IT system is the limitation of the scan range that can be selected once the parent ion is set; in our studies, species over 1020 amu were fragmented. Using the IT system described above, the product scan range resulted in a low-mass cut-off at *m/z* 285 amu. Because we also wanted to acquire information on fragments in the range between 250 and 280 amu, MS/MS was performed on the TQ system, analyzing in the product scan mode while the collision energy was set to 40V. All other parameters were identical to the setup described for the TQ system.

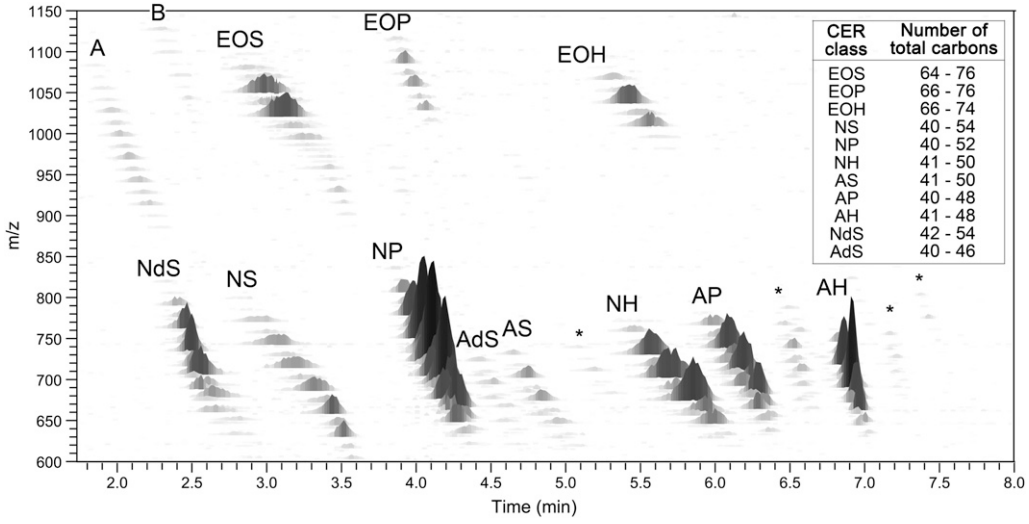

Fig. 3. Three-dimensional multi-mass chromatogram of dermatomed human SC. Positive ions of CER species using NPLC-APCI-MS. X-axis shows the retention time. Y-axis represents the *m/z* ratio (in amu). Z-axis depicts the relative intensity of the CER species. Classes noted by A, B, or * are unknown species. The inset in the upper right corner shows the range in which the various chain lengths of every CER class were observed.

High mass accuracy analysis

Accurate mass analysis of all synthetic CERs as well as the unidentified species observed in the lipid mixture isolated from native human SC was performed using a Fourier transform-ion cyclotron resonance (FT-ICR) system (LTQ FT Ultra, Thermo Electron) interfaced with a Surveyor LC pump and injector system equivalent to the one used for MS/MS analysis described above. The analysis time was set to 100 ms for mass accuracy up to four digits (deviation <1ppm) and the resolution was set at 100.000. All other parameters were comparable to the setup used for fragment analysis described above.

RESULTS AND DISCUSSION

Analysis and optimization of HPLC-APCI-MS

Prior to analysis of biological samples, the method was developed and optimized for all six synthetic CERs, resulting in applied parameters, which were described in the Materials and Methods section (Profiling of CERs in synthetic and biological mixtures). To analyze each individual synthetic CER with uniform chain length, NPLC was chosen over reverse phase LC because this mode allows for separation of individual CER subclasses. We chose to use a PVA column as it has advantages in terms of separation and peak shape compared with commonly used silica and diol columns (50, 51). Although ESI is mainly used for the analysis of CERs, the APCI mode is also used frequently. The latter permits a higher flow rate (in our studies, 0.8 ml/min) that results in a significantly shorter elution time of the CERs (43), thereby decreasing the overall LC/MS analysis time. The total ion chromatogram of the synthetic CERs is provided in **Fig. 2A** and shows that with this high flow rate, the CER subclasses are excellently separated. Because APCI was used, only single positively charged ions were present and could, under our conditions, be identified as either $[M+H]^+$ or $[M+H-H_2O]^+$ ions. The LOD and LOQ of all six synthetic CERs were determined and are listed in **Table 2**. These were calculated from ion extracted chromatograms obtained from full scan MS (*m/z* 600-1200 amu). The LOD and LOQ were defined by the signal-to-noise ratio (S/N), being 3 and 10, respectively.

This LC/MS method shows several advantages over others with regard to analysis time, sample preparation, and sensitivity. Qualitative analysis as well as relative comparability studies may be carried out easily. However, complete quantitative analysis of CERs is only possible when the effect of different ionization efficiencies between CER subclasses and chain lengths has been studied. Moreover, ion suppression effects (although they are expected to be of limited effect during APCI-MS) as well as sample preparation effects should also be taken into account. Ideally, each analyte should have its own isotopically labeled internal standards (C^{13}, N^{15}, and D^2 isotopes) added at different stages of the sample preparation and the analysis. This should allow for correction of the mentioned effects resulting in quantitative data of these CERs. However, such internal standards are not, or very limitedly, available. Therefore, a practical approach is to use a limited number of such standards that correct for these effects per CER subclass. Future studies will include several of these standards to make this assay (semi-) quantitative. The use of several nonisotopically labeled internal standards to correct for chain length and CER subclass regarding human SC is described in the literature only once (23).

CER analysis of human SC

To separate and analyze the CER subclasses from isolated human SC, a crude human SC lipid mixture was

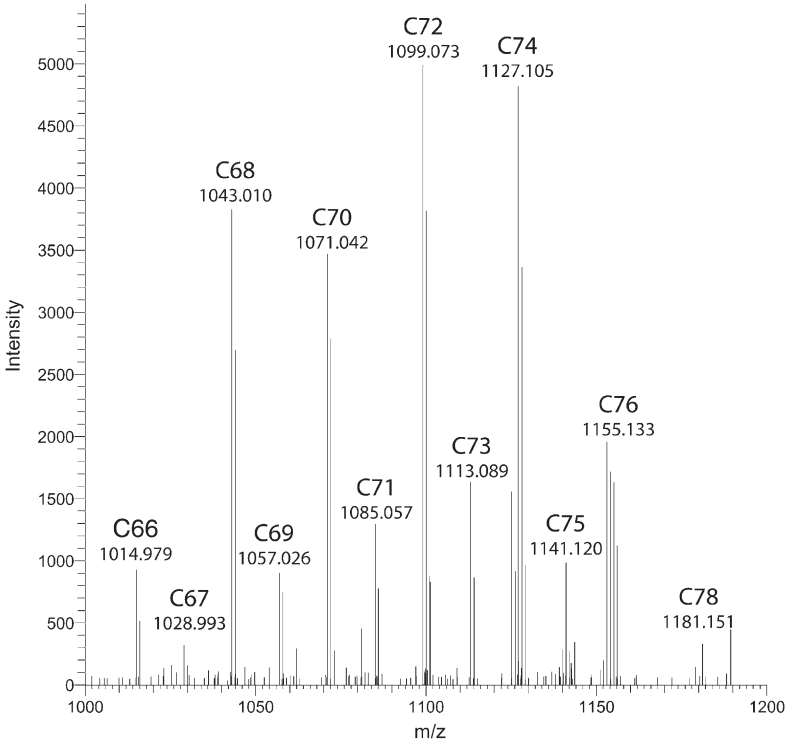

Fig. 4. Average mass spectrum (retention time range: 2.1–2.7 min; positive ion mode) of unidentified lipid class, performed by high mass accuracy FT-ICR MS. C-numbers correspond to the theoretical total number of carbon atoms the species should bear, i.e., the chain length of the proposed CER [EOdS].

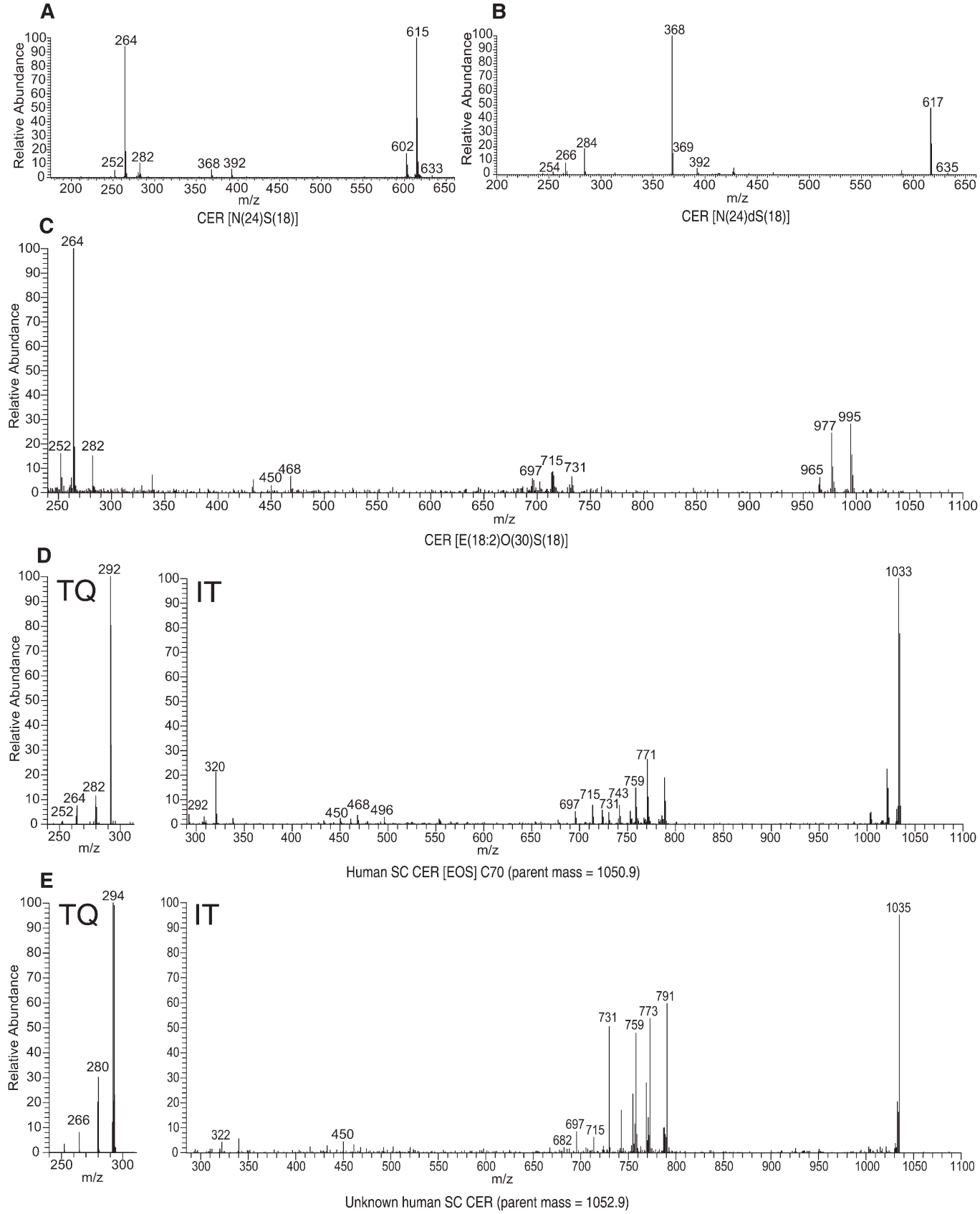

Fig. 5. MS/MS spectra of synthetic CERs using an ion trap (IT) system: (A) CER [N(18)S(24)]; (B) CER [N(18)dS(24)]; (C) CER E(18:2)O(30)S(18)]; (D) human SC CER subclass [EOS] C70, parent *m/z* 1050.9 amu; (E) unknown human SC CER, parent *m/z* 1052.9 amu. Because of the low *m/z* cut off and range limitations of MS/MS using an IT system (see text), a triple quadrupole (TQ) MS was used to obtain fragment ion spectra in the low mass range (250–300 amu) of human SC CER [EOS] (D) and the unknown CER (E).

injected using an identical setup as was used for synthetic CERs. The CER total ion chromatogram of the human SC sample is shown in Fig. 2B and shows elution and group separation of all CER subclasses within 8 min. The chromatographic resolution of the peaks was considerably lower compared with the synthetic CER mixture. This, however, can be fully explained by the presence of a wide range of both fatty acid and sphingosine chain lengths in each CER subclass, resulting in a relatively broad chromatographic peak per class; the total carbon chain length of the CER has a small effect on the polarity of the species thereby changing the retention time slightly. For example, both synthetic [N(18)P(24)] and its human SC counterpart elutes at 4.10 min and show similar peak shapes (Fig. 2A and supplementary Fig. I). However, human CER [NP] with a total chain length of 54 carbon atoms elutes at 3.72 min, whereas a total chain length of 40 shows a retention time at 4.18 min. This illustrates that the distribution in total number of carbon atoms results in the broadening of the total ion current peak as depicted in Fig. 2B. Nevertheless, this apparent 'loss in resolution' can be fully overcome by adding the *m/z* axis as a third dimension. The peaks that did show overlap in the human CERs total ion current chromatogram can therefore easily be distinguished in the 3D multi-mass chromatogram as shown in **Fig. 3**. This plot shows each separated CER class with multiple peaks from which each total carbon chain length could be derived. From this 3D plot, the variation in chain lengths and, therefore, the slight difference in polarity (i.e., retention time) can be seen clearly. An overview of the total carbon chain lengths of all CER subclasses is listed in the inset of Fig. 3. The calculated total chain length distribution is in line with those reported by Masukawa et al. (20). However, due to the high sensitivity of our method and the specific tuning for high mass CERs, it shows an even broader range of chain lengths for, in particular, the 'EO' subclasses. This results in the detection of CER subclasses with molecular masses over 1,100 amu corresponding to very long total carbon chain lengths up to 76 carbon atoms.

MS/MS of the unknown CER class

Besides 11 CER subclasses known to be present in human SC, Fig. 3 also shows the presence of other lipid subclasses, marked as *, A, and B, which are unidentified so far. Currently, four sphingoid base chains and three acyl chain variations have been indentified in CERs isolated from human SC, which results in, theoretically, 12 different CER subclasses (Fig. 1) (23, 39). CER [EOdS] has been previously observed by gas-liquid chromatography in pig skin and epidermal cysts as a variant of CER [EOS] (16, 52). However, its presence in human SC as a separate subclass has never been confirmed and recent literature on human SC only mentions 11 different subclasses, not pointing out CER [EOdS]. Therefore, our aim was to seek for the presence of this CER subclass [EOdS] in the 3D mass chromatogram. Becuase this CER bears an esterified fatty acid, its *m/z* value should be in the range of other [EO] subclasses (i.e., over 900 amu). Figure 3 depicts two unidentified lipid classes located in this high *m/z* range, A and B. To obtain more information about the unknown classes, LC-FT-ICR MS was used to determine the *m/z* of all peaks of both unidentified classes with high mass accuracy. From the high mass accuracy data it was concluded that the masses of the unidentified group labeled B in Fig. 3 correspond to the theoretical masses of the CER subclass [EOdS], and a combined mass spectrum of this unknown lipid class is shown in **Fig. 4**, including the accurate masses and the total number of C-atoms the species should bear. Another indication that this unidentified lipid class may correspond to CER [EOdS] was obtained from the observed elution/retention times: It is expected that CER [EOdS] elutes prior to the [EOS] subclass, as [NdS] and [AdS] both elute prior to their unsaturated nonhydroxy and ω-hydroxy sphingosine analogs, [NS] and [AS] respectively. This expectation is in accordance to the elution sequence of the unknown CER class and CER [EOS]. Therefore, both on the basis of the close agreement between the theoretical mass of the expected compound and the observed exact mass with matching elemental formulae as well as their relative retention times, there is a strong indication that this unknown subclass is indeed the CER [EOdS].

To confirm the hypothesis that this unknown CER subclass is indeed the proposed CER [EOdS], MS/MS experiments were performed to obtain structural information on the fragments of both known as well as the unknown CERs. Because no synthetic variant of CER [EOdS] is commercially available, synthetic CERs, viz. [N(24)S(18)], [N(24)dS(18)], and [E(18:2)O(30)S(18)], were fragmented to obtain product ions that could be characteristic for their structure. This data was compared with that reported before (39, 53–58). Following the synthetic CERs, CER fragment-ions of relevant human SC were analyzed. Subsequently, the above derived fragmentation reactions were used to identify fragments of the unknown SC CER subclass. The results of these fragmentation studies are shown in **Fig. 5 A–E** and **Table 3** and will be explained below. [It is not in the scope of this publication to fully interpret the observed spectra and identify all observed (fragment-) ions, as this requires additional studies.]

When focusing on the synthetic CER N(24)S(18) (Fig. 5A), very characteristic fragments were observed for both the sphingosine base as well as the fatty acid chain, which have also been reported in earlier studies (39, 54, 56, 58). In particular, fragments at *m/z* 252.3, 264.3, and 282.2 amu corresponding to $[(M+H)\text{-(FA chain)-}CH_3OH]^+$, $[(M+H)\text{-(FA chain)-}H_2O]^+$, and $[(M+H)\text{-(FA chain)}]^+$, respectively, are descriptive for a sphingosine base of 18 carbon atoms. Also, a fatty acid chain of 24 carbon atoms shows typical fragments at *m/z* 368.3 and 392.4 amu, which can be recognized as $[(M+H)\text{-(Sphingosine chain)}]^+$ and $[(M+H)\text{-}(C_{16}H_{31}OH)]^+$, respectively. Also, fragments without individual chain length information were observed; ions at *m/z* 602.4 and 614.6 amu, matching, respectively, $[(M+H)\text{-}H_2O\text{-}CH_3OH]^+$ and $[(M+H)\text{-}H_2O]^+$ ions, are also present in Fig. 5A. Subsequently, MS/MS experiments were conducted on CER [N(24)

dS(18)], resulting in the mass spectrum shown in Fig. 5B. Again, fragments corresponding to the fatty acid chain and the sphingosine base were observed (54, 56, 58); the fatty acid related fragments of CER [NdS] are similar to their CER [NS] counterparts (*m/z* 368.3 and 392.4 amu). This is expected because both structures contain a non-hydroxy fatty acid and are therefore identical. Fragments related to the sphingosine base are shifted +2 amu (*m/z* 254.3, 266.3, and 284.2 amu). This is also in agreement as CER [dS] contains one degree of saturation less, i.e., two hydrogen atoms more. Hereafter, the more complicated CER [EOS], consisting of a sphingosine base 18 carbon atoms long and a fatty acid chain 30 carbon atoms long with a linoleic acid moiety esterified to it, was studied. Fragmentation of this CER resulted in a mass spectrum present in Fig. 5C. Because this CER also bears a sphingosine base, fragments with respect to the sphingosine chain are similar to CER [NS] and CER [NdS] (viz., ions at *m/z* 252.3, 264.3, 282.2 amu). The fragments at *m/z* 450.5, 730.7, and 964.9 amu correspond to fragments related to the fatty acid chain. The MS/MS spectrum of CER [EOS] contains additional fragments compared with CER [NS] and [NdS] because the esterified linoleic acid may fragment as well. Fragments at *m/z* 696.7 and 714.7 amu indicate the loss of a linoleic moiety with and without the loss of a water molecule, respectively.

Subsequently, MS/MS spectra of the human SC variant of CER [EOS] were studied to confirm that their fragmentation is in agreement with these observations. The precursor ion of CER [E(18:2)O(34)S(18)] at *m/z* 1050.9 amu was fragmented and the result is shown in Fig. 5D. Indeed, fragments corresponding to the loss of the fatty acid chain, the sphingosine chain, as well as fragments without the ester chain were observed (see Table 3). In addition, fragments showed individual chain lengths of either the fatty acid or sphingosine chain. The characteristic sphingosine fragment of *m/z* 264.3 amu, for example (C18 sphingosine), also showed fragments of *m/z* 292.3 and 320.3 amu (respectively, C20 and C22). The same phenomenon was observed for esterified fatty acid fragments like 730.7 and 758.7 (C48 and C50). Finally, we performed MS/MS on the hypothesized CER [EOdS] observed in human SC. Because human CER contains various chain lengths in a single subclass, the precursor ion of the proposed CER [E(18:2)O(34)dS(18)], at *m/z* 1052.9 was selected for fragmentation studies. This precursor ion should, following observations described above, lead to fragments best comparable to the CER [E(18:2)O(34)S(18)] counterpart.

TABLE 3. Overview of MS fragments of both synthetic and biological ceramides and its structural correlation

Ceramide subclass	Molecular structure including locations of possible fragmentation	m/z (amu)	Loss of functional group						
			H_2O	FA chain *1*	Sph chain *2*	CH_3OH *3*	$C_{16}H_{31}OH$ *4*	Ester chain *5*	*6*
[N(24)S(18)] Parent ion = 651 (synthetic)	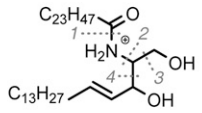	252		X		X			
		264	X	X					
		282		X					
		368			X				
		392					X		
		602	X			X			
		615	XX						
		633	X						
[N(24)dS(18)] Parent ion = 653 (synthetic)	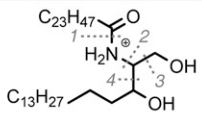	254		X		X			
		266	X	X					
		284		X					
		368			X				
		392					X		
		617	XX						
		635	X						
[E(18:2)O(30)S(18)] Parent ion = 1013 (synthetic)	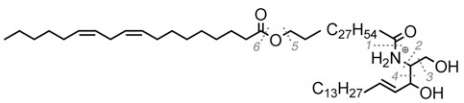	252		X		X			
		264	X	X					
		282		X					
		450			X			X	
		468			X				X
		697	XX					X	
		715	X					X	
		731			X				
		965	X			X			
		977	XX						
		995	X						
[EOS] C70, parent ion = 1051 (human SC)	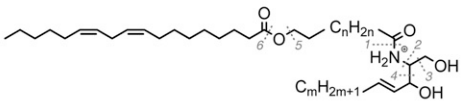	264/292/320[a, b]	X	X					
		282[a]		X					
		450			X			X	
		468/496			X				X
		697	XX					X	
		715/743/771[b]	X					X	
		731/759†			X				
		1033	XX						
[EOdS] (proposed) parent ion = 1053 (human SC)	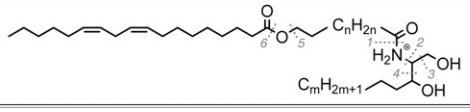	266/280/294/322[a, b]	X	X					
		450			X			X	
		731/759[b]			X				
		773	X					X	
		791	X						X
		1035	XX						

Dotted lines with their corresponding numbers depict the location of fragmentation, viz. which functional group is lost. The variables *m* and *n* located in the molecular structure indicate variations in chain length. FA chain, fatty acid chain; Sph chain, sphingosine chain. X indicates that the particular functional group is lost for that particular mass. XX means that functional group is lost twice.

[a] Indicates these fragments were measured using a triple quadrupole (TQ) system. All other fragments are observed using an ion trap (IT) mass spectrometer.

[b] Indicates that besides this particular *m/z* value, values that lost the same functional group but show different masses were observed. This is due to the variation in total chain length in human SC, so a different length in carbon backbone results in mass peaks located exactly one or more CH_2 masses shifted. For example, fragment *m/z* 280 amu lost the same functional group as 266 amu; the only difference is the chain length of the fatty acid backbone, which is one CH_2 group longer.

Figure 5E shows the MS/MS spectrum obtained from this precursor ion. Very indicative fragments, which were observed in both CER [EOS] as well as in CER [NdS], also appear in this spectrum, indicating that this unidentified species indeed contains an esterified ω-hydroxy fatty acid moiety and also bears a dihydrosphingosine chain (i.e., 266.3, 450.5, 730.7, 772.7, 790.8). This strongly supports the hypothesis that the unknown CER class is indeed CER [EOdS]. From Fig. 4, it can be concluded that the mass range of this newly identified CER [EOdS] ranges from *m/z* 1015.0 to 1181.1 amu and corresponds exactly with a CER [EOdS], having a total chain length ranging from 66 to 78 carbon atoms long. Besides, it is known from literature that the CERs containing an even number of carbon atoms are more abundantly present than odd chain length CERs (21, 23), which is also the case in our mass spectrum of Fig. 4, again confirming that the unknown CER subclass is CER [EOdS].

Finally, we also hypothesized on the possible molecular structure of the unknown lipid class noted as 'A' in Fig. 3. Although we cannot make any firm conclusion because no extensive MS/MS studies were performed, it can be pointed out that this lipid species bears a mass in similar ranges as the CER [EO] subclasses. Moreover, from the early elution time, it can be concluded that this lipid class is more apolar than all known CERs subclasses. **Figure 6** shows the mass spectrum result of high mass accuracy analysis performed on these species by FT-ICR MS, including the respective molecular formulae for every peak observed. These molecular formulae are quite conclusive, as the difference between the observed and theoretical mass is low, between −0.17 and 1.06 ppm. Although it is highly speculative what the molecular structure of this lipid class is, the arguments mentioned above, in combination with the exact mass data, may point to a lipid structure comparable to CER [EOdS] but with one OH-group less. More extensive research and repeated measurements will address this lipid in future studies.

Human skin CER analysis harvested by using tape strips

Our aim was to develop a method for CER analysis that could also provide a CER profile when harvesting in vivo SC using tape strips. Because tape strips usually contain substantial amounts of contaminants, like polymers, most of them are incompatible with LC/MS. To circumvent these issues, we decided to use poly(phenylene sulfide) tape strips obtained from Nichiban. These tape strips were also used in studies for CER analysis by Masukawa et al. (23, 39). After lipid extraction and the additional concentration step (see Material and Methods), samples were injected and the 3D CER profile is shown in **Fig. 7**. All the CER subclasses with varying chain length distributions could be identified and possible contaminants from the tape did not interfere with the results. All known CER classes can be observed in tape strip-harvested SC and only minor deviations from the profile were observed. The nature of these differences remains to be investigated in future studies.

CER analysis of a human skin explant model

The extracted lipids from a cultured full-thickness skin explants model were analyzed using the same method as used for dermatomed skin and skin harvested from tape strips. The results of the two individual pools were comparable and one of these 3D multi-mass chromatograms is presented in Fig. 7B. Although it is not the purpose of this study to thoroughly investigate the exact differences between human skin and the cultured full-thickness skin explant model, from Fig. 7B it can be concluded that this model contains several differences, including additional lipid subclasses compared with native human skin, possibly CERs.

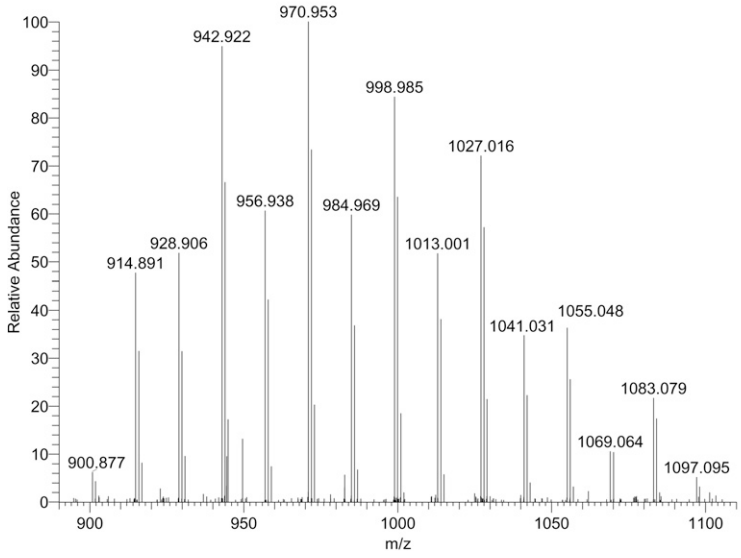

m/z	Composition	Delta (ppm)
900.876	C59 H114 O4 N	0.92
914.891	C60 H116 O4 N	0.24
928.906	C61 H118 O4 N	-0.04
942.922	C62 H120 O4 N	0.15
956.938	C63 H122 O4 N	0.45
970.953	C64 H124 O4 N	0.32
984.969	C65 H126 O4 N	0.32
998.985	C66 H128 O4 N	0.95
1013.001	C67 H130 O4 N	0.65
1027.016	C68 H132 O4 N	0.30
1041.031	C69 H134 O4 N	-0.17
1055.048	C70 H136 O4 N	0.94
1069.064	C71 H138 O4 N	1.06
1083.079	C72 H140 O4 N	0.62
1097.095	C73 H142 O4 N	0.89

Fig. 6. Average mass spectrum (retention time range: 1.8–2.4 min; positive ion mode) of unidentified lipid class, performed by high mass accuracy FT-ICR MS, including mass table with the differences (Delta) of the observed and theoretical mass of the proposed molecular formulae in ppm (ppm).

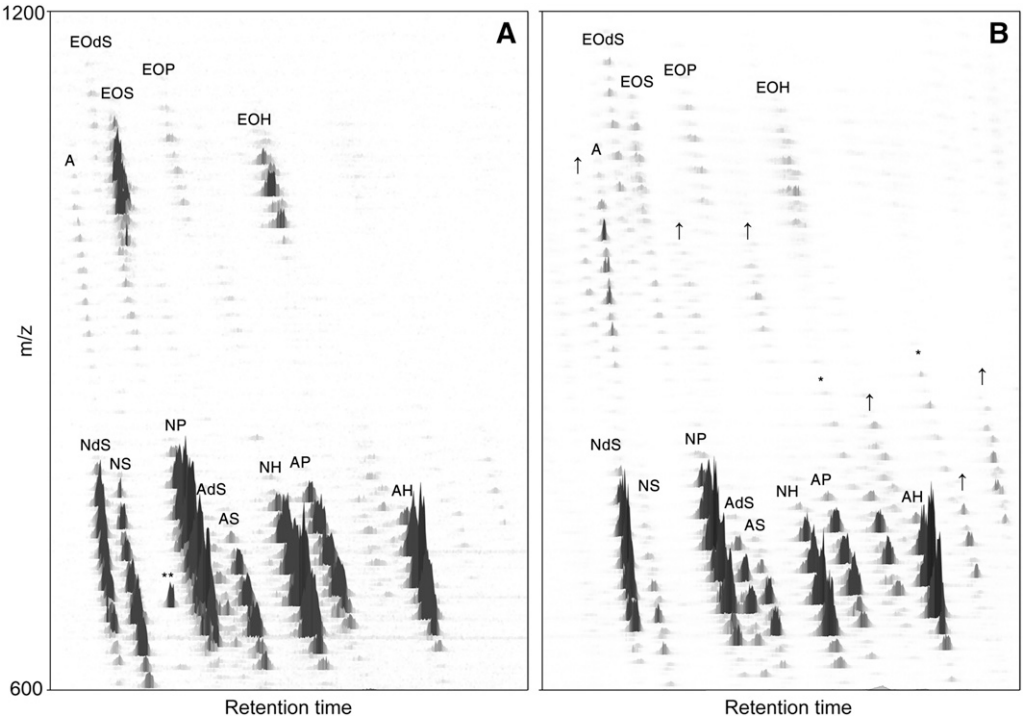

Fig. 7. Three-dimensional multi-mass chromatogram of (A) tape strips from human SC; (B) cultured full-thickness skin explants. "A" respresent the same unknown lipid mass as was shown in human SC from dermatomed skin (Figure 3). Compared with human SC from dermatomed skin, some lipid species in cultured full-thickness skin explants show either higher abundance (noted by ↑), or did not show up in dermatomed skin at all and might therefore possibly be different CER species (noted by *). Probable contaminants caused by the tape strip are depicted as **.

CONCLUSION

In this paper, we describe a new method for effectively profiling SC CERs with high sensitivity and only a very limited number of sample preparation steps, making this method very approachable for the analysis of different sorts of SC samples. The high sensitivity of our method, in particular for CERs with a higher mass range, resulted in the detection of additional lipid classes of which one could be identified as CER [EOdS]. This is the fourth CER linoleic moiety esterified to a very long fatty acid chain confirmed to be present in human skin by LC/MS. We also successfully applied this method to CERs extracted from human SC harvested using tape strips. Because low quantities of lipids are obtained by tape stripping, an LC/MS method with high sensitivity is required. Also regarding these tape strip samples, the developed method was robust enough to detect all CERs. Finally, samples from a cultured full-thickness skin explant model could also be analyzed using this developed method and sensitivity seems no issue. Future research on CER analysis may benefit from this new method, showing an easy, robust, quick, and sensitive method for analysis of these lipid species.

The authors would like to thank Robert Rissmann and Judith van Dommellen for their contribution to the development of the LC/MS method, and Varsha Thakoersing for providing cultured full-thickness skin explants.

REFERENCES

1. Madison, K. C. 2003. Barrier function of the skin: "la raison d'etre" of the epidermis. *J. Invest. Dermatol.* **121:** 231–241.
2. Wertz, P. W., and B. van den Bergh. 1998. The physical, chemical and functional properties of lipids in the skin and other biological barriers. *Chem. Phys. Lipids.* **91:** 85–96.
3. Coderch, L., O. Lopez, A. de la Maza, and J. L. Parra. 2003. Ceramides and skin function. *Am. J. Clin. Dermatol.* **4:** 107–129.
4. Elias, P. M., and D. S. Friend. 1975. The permeability barrier in mammalian epidermis. *J. Cell Biol.* **65:** 180–191.
5. Di Nardo, A., P. Wertz, A. Giannetti, and S. Seidenari. 1998. Ceramide and cholesterol composition of the skin of patients with atopic dermatitis. *Acta Derm. Venereol.* **78:** 27–30.
6. Farwanah, H., K. Raith, R. H. Neubert, and J. Wohlrab. 2005. Ceramide profiles of the uninvolved skin in atopic dermatitis and psoriasis are comparable to those of healthy skin. *Arch. Dermatol. Res.* **296:** 514–521.
7. Imokawa, G., A. Abe, K. Jin, Y. Higaki, M. Kawashima, and A. Hidano. 1991. Decreased level of ceramides in stratum corneum of atopic dermatitis: an etiologic factor in atopic dry skin? *J. Invest. Dermatol.* **96:** 523–526.
8. Ishikawa, J., H. Narita, N. Kondo, M. Hotta, Y. Takagi, Y. Masukawa, T. Kitahara, Y. Takema, S. Koyano, S. Yamazaki, et al. 2010. Changes in the ceramide profile of atopic dermatitis patients. *J. Invest. Dermatol.* **130:** 2511–2514.
9. Raith, K., H. Farwanah, S. Wartewig, and R. H. H. Neubert. 2004. Progress in the analysis of stratum corneum ceramides. *Eur. J. Lipid Sci. Technol.* **106:** 561–571.
10. Jungersted, J. M., L. I. Hellgren, G. B. E. Jemec, and T. Agner. 2008. Lipids and skin barrier function - a clinical perspective. *Contact Dermatol.* **58:** 255–262.
11. Jungersted, J. M., H. Scheer, M. Mempel, H. Baurecht, L. Cifuentes, J. K. Hogh, L. I. Hellgren, G. B. E. Jemec, T. Agner, and S. Weidinger. 2010. Stratum corneum lipids, skin barrier function and filaggrin mutations in patients with atopic eczema. *Allergy.* **65:** 911–918.

12. Ponec, M., A. Weerheim, P. Lankhorst, and P. Wertz. 2003. New acylceramide in native and reconstructed epidermis. *J. Invest. Dermatol.* **120:** 581–588.
13. Robson, K. J., M. E. Stewart, S. Michelsen, N. D. Lazo, and D. T. Downing. 1994. 6-Hydroxy-4-sphingenine in human epidermal ceramides. *J. Lipid Res.* **35:** 2060–2068.
14. Stewart, M. E., and D. T. Downing. 1995. Free sphingosines of human skin include 6-hydroxysphingosine and unusually long-chain dihydrosphingosines. *J. Invest. Dermatol.* **105:** 613–618.
15. Stewart, M. E., and D. T. Downing. 1999. A new 6-hydroxy-4-sphingenine-containing ceramide in human skin. *J. Lipid Res.* **40:** 1434–1439.
16. Wertz, P. W., and D. T. Downing. 1983. Ceramides of pig epidermis: structure determination. *J. Lipid Res.* **24:** 759–765.
17. Higuchi, H., M. Nakamura, A. Kuwano, M. Kasamatsu, and H. Nagahata. 2005. Quantities and types of ceramides and their relationships to physical properties of the horn covering the claws of clinically normal cows and cows with subclinical laminitis. *Can. J. Vet. Res.* **69:** 155–158.
18. Shimada, K., J. S. Yoon, T. Yoshihara, T. Iwasaki, and K. Nishifuji. 2009. Increased transepidermal water loss and decreased ceramide content in lesional and non-lesional skin of dogs with atopic dermatitis. *Vet. Dermatol.* **20:** 541–546.
19. Farwanah, H., B. Pierstorff, C. E. Schmelzer, K. Raith, R. H. Neubert, T. Kolter, and K. Sandhoff. 2007. Separation and mass spectrometric characterization of covalently bound skin ceramides using LC/APCI-MS and Nano-ESI-MS/MS. *J. Chromatogr. B Analyt. Technol. Biomed. Life Sci.* **852:** 562–570.
20. Farwanah, H., J. Wirtz, T. Kolter, K. Raith, R. H. Neubert, and K. Sandhoff. 2009. Normal phase liquid chromatography coupled to quadrupole time of flight atmospheric pressure chemical ionization mass spectrometry for separation, detection and mass spectrometric profiling of neutral sphingolipids and cholesterol. *J. Chromatogr. B Analyt. Technol. Biomed. Life Sci.* **877:** 2976–2982.
21. Farwanah, H., J. Wohlrab, R. H. Neubert, and K. Raith. 2005. Profiling of human stratum corneum ceramides by means of normal phase LC/APCI-MS. *Anal. Bioanal. Chem.* **383:** 632–637.
22. Masukawa, Y., H. Narita, and G. Imokawa. 2005. Characterization of the lipid composition at the proximal root regions of human hair. *J. Cosmet. Sci.* **56:** 1–16.
23. Masukawa, Y., H. Narita, H. Sato, A. Naoe, N. Kondo, Y. Sugai, T. Oba, R. Homma, J. Ishikawa, Y. Takagi, et al. 2009. Comprehensive quantification of ceramide species in human stratum corneum. *J. Lipid Res.* **50:** 1708–1719.
24. Masukawa, Y., and H. Tsujimura. 2007. Highly sensitive determination of diverse ceramides in human hair using reversed-phase high-performance liquid chromatography-electrospray ionization mass spectrometry. *Lipids.* **42:** 275–290.
25. Vietzke, J. P., O. Brandt, D. Abeck, C. Rapp, M. Strassner, V. Schreiner, and U. Hintze. 2001. Comparative investigation of human stratum corneum ceramides. *Lipids.* **36:** 299–304.
26. Hinder, A., C. E. Schmelzer, A. V. Rawlings, and R. H. Neubert. 2011. Investigation of the molecular structure of the human stratum corneum ceramides [NP] and [EOS] by mass spectrometry. *Skin Pharmacol. Physiol.* **24:** 127–135.
27. Raith, K., and R. H. H. Neubert. 2000. Liquid chromatography-electrospray mass spectrometry and tandem mass spectrometry of ceramides. *Anal. Chim. Acta.* **403:** 295–303.
28. Cremesti, A. E., and A. S. Fischl. 2000. Current methods for the identification and quantitation of ceramides: an overview. *Lipids.* **35:** 937–945.
29. Hannun, Y. A., and L. M. Obeid. 2008. Principles of bioactive lipid signalling: lessons from sphingolipids. *Nat. Rev. Mol. Cell Biol.* **9:** 139–150.
30. Taha, T. A., T. D. Mullen, and L. M. Obeid. 2006. A house divided: ceramide, sphingosine, and sphingosine-1-phosphate in programmed cell death. *Biochim. Biophys. Acta.* **1758:** 2027–2036.
31. Kitatani, K., J. Idkowiak-Baldys, and Y. A. Hannun. 2008. The sphingolipid salvage pathway in ceramide metabolism and signaling. *Cell. Signal.* **20:** 1010–1018.
32. Vaena de Avalos, S., J. A. Jones, and Y. A. Hannun. 2004. Ceramides. *In* Bioactive Lipids. A. Nicolaou and G. G. Kokotos, editors. The Oily Press, Bridgwater. 135–167.
33. Jayadev, S., B. Liu, A. E. Bielawska, J. Y. Lee, F. Nazaire, M. Pushkareva, L. M. Obeid, and Y. A. Hannun. 1995. Role for ceramide in cell cycle arrest. *J. Biol. Chem.* **270:** 2047–2052.
34. Hannun, Y. A., and C. Luberto. 2000. Ceramide in the eukaryotic stress response. *Trends Cell Biol.* **10:** 73–80.
35. Kolesnick, R. N., and M. Kronke. 1998. Regulation of ceramide production and apoptosis. *Annu. Rev. Physiol.* **60:** 643–665.
36. Riboni, L., A. Prinetti, R. Bassi, A. Caminiti, and G. Tettamanti. 1995. A mediator role of ceramide in the regulation of neuroblastoma Neuro2a cell differentiation. *J. Biol. Chem.* **270:** 26868–26875.
37. Venable, M. E., J. Y. Lee, M. J. Smyth, A. Bielawska, and L. M. Obeid. 1995. Role of ceramide in cellular senescence. *J. Biol. Chem.* **270:** 30701–30708.
38. Pena, L. A., Z. Fuks, and R. Kolesnick. 1997. Stress-induced apoptosis and the sphingomyelin pathway. *Biochem. Pharmacol.* **53:** 615–621.
39. Masukawa, Y., H. Narita, E. Shimizu, N. Kondo, Y. Sugai, T. Oba, R. Homma, J. Ishikawa, Y. Takagi, T. Kitahara, et al. 2008. Characterization of overall ceramide species in human stratum corneum. *J. Lipid Res.* **49:** 1466–1476.
40. Jessome, L. L., and D. A. Volmer. 2006. Ion suppression: a major concern in mass spectrometry. Advanstar Communications, Duluth, MN. 498–511.
41. Matuszewski, B. K., M. L. Constanzer, and C. M. Chavez-Eng. 1998. Matrix effect in quantitative LC/MS/MS analyses of biological fluids: a method for determination of finasteride in human plasma at picogram per milliliter concentrations. *Anal. Chem.* **70:** 882–889.
42. Bruins, C. H., C. M. Jeronimus-Stratingh, K. Ensing, W. D. van Dongen, and G. J. de Jong. 1999. On-line coupling of solid-phase extraction with mass spectrometry for the analysis of biological samples. I. Determination of clenbuterol in urine. *J. Chromatogr. A.* **863:** 115–122.
43. de Hoffmann, E., and V. Stroobant. 2007. Mass Spectrometry, Principles and Applications. 3rd ed. Wiley, Chichester, UK.
44. Ashcroft, A. E. 1997. Atmospheric pressure chemical ionization. *In* Ionization Methods in Organic Mass Spectrometry. N. W. Barnett, editor. The Royal Society of Chemistry, Cambridge (UK).
45. Lebonvallet, N., C. Jeanmaire, L. Danoux, P. Sibille, G. Pauly, and L. Misery. 2010. The evolution and use of skin explants: potential and limitations for dermatological research. *Eur. J. Dermatol.* **20:** 671–684.
46. Motta, S., M. Monti, S. Sesana, R. Caputo, S. Carelli, and R. Ghidoni. 1993. Ceramide composition of the psoriatic scale. *Biochim. Biophys. Acta.* **1182:** 147–151.
47. Nugroho, A. K., L. Li, D. Dijkstra, H. Wikström, M. Danhof, and J. A. Bouwstra. 2005. Transdermal iontophoresis of the dopamine agonist 5-OH-DPAT in human skin in vitro. *J. Control. Release.* **103:** 393–403.
48. Bligh, E. G., and W. J. Dyer. 1959. A rapid method of total lipid extraction and purification. *Can. J. Biochem. Physiol.* **37:** 911–917.
49. Thakoersing, V. S., M. Ponec, and J. A. Bouwstra. 2010. Generation of human skin equivalents under submerged conditions-mimicking the in utero environment. *Tissue Eng. Part A.* **16:** 1433–1441.
50. Christie, W. W., S. Gill, J. Nordbäck, Y. Itabashi, S. Sanda, and A. R. Slabas. 1998. New procedures for rapid screening of leaf lipid components from Arabidopsis. *Phytochem. Anal.* **9:** 53–57.
51. Quinton, L., K. Gaudin, A. Baillet, and P. Chaminade. 2006. Microanalytical systems for separations of stratum corneum ceramides. *J. Sep. Sci.* **29:** 390–398.
52. Wertz, P. W., D. C. Swartzendruber, K. C. Madison, and D. T. Downing. 1987. Composition and morphology of epidermal cyst lipids. *J. Invest. Dermatol.* **89:** 419–425.
53. Schiffmann, S., J. Sandner, K. Birod, I. Wobst, C. Angioni, E. Ruckhaberle, M. Kaufmann, H. Ackermann, J. Lotsch, H. Schmidt, et al. 2009. Ceramide synthases and ceramide levels are increased in breast cancer tissue. *Carcinogenesis.* **30:** 745–752.
54. Masukawa, Y., H. Tsujimura, and H. Narita. 2006. Liquid chromatography-mass spectrometry for comprehensive profiling of ceramide molecules in human hair. *J. Lipid Res.* **47:** 1559–1571.
55. Hsu, F. F., J. Turk, M. E. Stewart, and D. T. Downing. 2002. Structural studies on ceramides as lithiated adducts by low energy collisional-activated dissociation tandem mass spectrometry with electrospray ionization. *J. Am. Soc. Mass Spectrom.* **13:** 680–695.
56. Yoo, H. H., J. Son, and D. H. Kim. 2006. Liquid chromatography-tandem mass spectrometric determination of ceramides and related lipid species in cellular extracts. *J. Chromatogr. B Analyt. Technol. Biomed. Life Sci.* **843:** 327–333.
57. Schiffmann, S., J. Sandner, R. Schmidt, K. Birod, I. Wobst, H. Schmidt, C. Angioni, G. Geisslinger, and S. Grosch. 2009. The selective COX-2 inhibitor celecoxib modulates sphingolipid synthesis. *J. Lipid Res.* **50:** 32–40.
58. Shaner, R. L., J. C. Allegood, H. Park, E. Wang, S. Kelly, C. A. Haynes, M. C. Sullards, and A. H. Merrill, Jr. 2009. Quantitative analysis of sphingolipids for lipidomics using triple quadrupole and quadrupole linear ion trap mass spectrometers. *J. Lipid Res.* **50:** 1692–1707.